Advances in Science and Technology Research Journal

Advances in Science and Technology Research Journal, 2026, 20(3), 387–395
https://doi.org/10.12913/22998624/214298
ISSN 2299-8624, License CC-BY 4.0

Received: 2025.09.27
Accepted: 2025.12.16
Published: 2026.02.01

Multi-objective optimization of the slide burnishing process for 36CrNiMo4 steel using the topsis approach

Andrzej Dzierwa[1*], Jan Slota[2], Angelos Markopoulos[3]

[1] Faculty of Mechanical Engineering and Aeronautics, Rzeszow University of Technology, al. Powstancow Warszawy 8, 35-959 Rzeszow, Poland
[2] Faculty of Mechanical Engineering, Technical University of Kosice, Letná 9, 042 00 Sever, Kosice, Slovakia
[3] School of Mechanical Engineering, National Technical University of Athens, Ir. Politechniou 9, Zografou 157 80, Athens, Greece
* Corresponding author's e-mail: adzierwa@prz.edu.pl

ABSTRACT

The research presents a multi-objective optimization of the slide burnishing process applied to 36CrNiMo4 steel, aiming to enhance surface quality and mechanical properties. The study focuses on key process parameters, including burnishing force, feed rate, and burnishing speed, and their effects on surface roughness, microhardness, and residual stress. The technique for order preference by similarity to ideal solution (TOPSIS) approach is employed to identify optimal parameter settings that balance multiple objectives simultaneously. The conducted research demonstrates significant improvements in the treated steel components and the process parameters: P = 120 N, f = 0.04 mm/rev, n = 900 rev/min were found to be the most advantageous. The proposed optimization framework provides an effective decision-making tool for process engineers to achieve superior surface integrity in slide burnishing applications.

Keywords: slide burnishing, surface topography, TOPSIS method, multi-objective optimization.

INTRODUCTION

Unlike conventional smoothing methods (polishing, honing, lapping), smoothing-strengthening machining not only enhances shape and dimensional accuracy but also imparts specific surface characteristics that positively influence the operational properties of the workpieces [1]. Smoothing-strengthening processing enhances surface hardness, achieves excellent smoothness, introduces compressive stresses, shapes the desired surface topography, and eliminates abrasive contamination typical of abrasive processing methods. This category includes various types of burnishing, such as ball burnishing [2], disc burnishing [3], texturing burnishing [4], roller burnishing [5] and even the techniques like shot peening [6]. Slide burnishing is a surface finishing technique that enhances a workpiece's surface by inducing plastic deformation. This is achieved by pressing and sliding a hard tool against the surface, generating compressive force and friction to smooth out irregularities [7]. Diamond is recommended as a burnishing tool; however, for economic reasons, it is often successfully replaced by ceramic materials. The key input parameters of slide burnishing that significantly affect the final results include [7]:

- Tool-related parameters: burnishing force, burnishing tool material, tool geometry and shape,
- Process parameters: burnishing speed, feed rate, number of passes, lubrication and cooling,
- Workpiece-related parameters: material type and hardness, initial surface roughness, workpiece geometry and stiffness.

Dyl et al. [8] conducted tests on the slide burnishing of X2CrNiMo17-12-2 steel. They demonstrated that, with the appropriate processing parameters, surface quality significantly improved by reducing surface roughness and hardening the

surface layer. Additionally, the process oriented the microstructure grains towards deformation, enhancing the material's efficiency and durability. Márquez-Herrera et al. [9] applied the slide burnishing process to advanced high-strength steels TRIP-440Y and DP-330Y, as well as the high-strength steel HSLA-SP780. The tests showed that, depending on the burnishing force, roughness amplitude parameters were reduced by 2.8% to 83.2%. Meanwhile, corrosion tests indicated that slide burnishing does not significantly affect the corrosion resistance of steels coated with a zinc layer. The positive effect of burnishing on reducing selected surface topography parameters was also demonstrated by the Tesfom et al. [10], and Felhő et al. [11], who identified the optimal input process parameters for this purpose. Zaghal et al. [12] reported that diamond burnishing of 42CrMo4 steel significantly enhances surface quality by reducing surface roughness, introducing residual compressive stresses, and increasing microhardness. This process also improved the microstructure, ultimately leading to better fatigue life compared to surfaces finished solely by hard turning or grinding. Kuznetsov et al. [13] found that slide burnishing significantly improved the surface quality of 03Cr16Ni15Mo3Ti1 austenitic stainless steel by reducing roughness parameters. The smoothing coefficient achieved 79–90%, with the average roughness decreasing from 1.0 to 0.1 µm. Surface hardness also increased by 15% to 43%, depending on the applied normal force. Korzynski et al. [14] analyzed the influence of the slide burnishing process on the condition of the surface layer of valve stems made of 317Ti steel. The results revealed an increase in microhardness by approximately 25% and compressive stress by about 60%, which resulted in increased durability of the valve stems. A significant improvement in the surface quality of AISI 316Ti steel was also observed by the Maximov et al. [15]. The researchers obtained a roughness parameter (Ra) value of 0.055 µm and an increase in microhardness by over 32%. Moreover, the application of the slide burnishing process led to a 38.9% enhancement in fatigue strength, as well as improved wear resistance and residual stress characteristics.

In recent years, multi-criteria decision-making (MCDM) methods have attracted increasing interest, and one of the most widely used among them is the TOPSIS method. For example, the authors of [16] used it for the selection of boron-based tribological hard coatings, while Khan et al. [17] applied it to determine the effects of applied load, abrasion distance, and TiC content on wear rate, coefficient of friction, and frictional heating during the wear process of TiC-reinforced zinc–aluminum composites. Similarly, Thirumalvalavan et al. [18] applied TOPSIS to optimize HVOF coating parameters for WC–Co nanocoatings on Ti-6Al-4V alloy.

Previous studies have mainly focused on assessing the influence of slide burnishing on individual output parameters, such as roughness, microhardness, and stress. However, there is a lack of comprehensive approach to selecting the values of individual input parameters while simultaneously considering multiple output factors in a specified percentage. This article aims to fill this gap by using the TOPSIS method (the Technique for Order of Preference by Similarity to Ideal Solution) to select the optimal input parameters for the slide burnishing process, taking multiple output parameters into account simultaneously.

METHODS

The slide burnishing process was carried out using a TUJ-50M conventional lathe. The test material consisted of shafts made of 36CrNiMo4 steel with a hardness of 42±2 HRC. The burnishing element in the form of a 6.35 mm diameter ball was made of tungsten carbide (WC) with a hardness of 70±2 HRC. The roughness Ra of the balls was 0.35 µm. The input parameters of the process were the burnishing force, feed and rotational speed. A single tool pass was assumed in the tests. Table 1 presents the matrix with combinations of levels for individual input parameters of the process according to the L18 Taguchi orthogonal plan. All discs were turned before burnishing using a carbide insert with the following turning parameters: v_c = 140 m/min, f = 0.10 mm/rev, a_p = 0.3 mm and its map as well as the selected surface topography parameters according to PN-EN ISO 25178-2:2012 [19] are presented in Figure 1. The initial surface after finish turning exhibited an average areal roughness of Sa = 0.82 ± 0.05 µm, measured at seven locations. Surface topography of slide burnished discs was measured using white light interferometer Talysurf CCI Lite. The measuring area for each variant was 3 × 3 mm. After each measurement, the surface topography parameters were calculated using TalyMap software, following the methodology in [20]. Microhardness

Table 1. Slide burnishing input parameters

No.	P [N]	f [mm/rev]	n [rev/min]
SB_01	15	0.04	300
SB_02	15	0.08	600
SB_03	15	0.12	900
SB_04	50	0.04	300
SB_05	50	0.08	600
SB_06	50	0.12	900
SB_07	85	0.04	600
SB_08	85	0.08	900
SB_09	85	0.12	300
SB_10	120	0.04	900
SB_11	120	0.08	300
SB_12	120	0.12	600
SB_13	155	0.04	600
SB_14	155	0.08	900
SB_15	155	0.12	300
SB_16	190	0.04	900
SB_17	190	0.08	300
SB_18	190	0.12	600

measurements were performed using a Brivisor KL2 microhardness tester with HME measuring electronics, applying the Vickers static indenter pressing method at a constant load of P = 4.9 N. The indenter, shaped as a regular quadrangular pyramid with a dihedral angle of 136°, was applied for approximately 15 seconds. The microhardness of the surface layer of the tested samples was measured on oblique sections made at an angle of 5°.

Residual stresses were measured using a portable X-ray diffractometer, Xstress 3000 G3R. The $\sin^2\psi$ method [21] was employed, with the incidence angle ψ varying from −45° to +45°, divided into seven tilt positions. The exposure time was set to 40 seconds, with a penetration depth of approximately 10 μm. XTronic software was applied for the measurements. For each sample, residual stresses were determined in two directions: perpendicular and parallel to the machining marks. Each measurement was repeated three times, and the mean values with Type A standard uncertainty (calculated from the standard deviation) are reported.

A multi-criteria decision-making tool – TOPSIS method was selected in other to optimize slide burnishing machining parameters taking into account three output parameters - roughness, microhardness, and residual stresses. The calculation procedure consists of the following steps [22, 23]:

1. Creation of a normalized data matrix according to the formula:

$$n_{ij} = \frac{x_{ij}}{\sqrt{\sum_{i=1}^{m} x_{ij}^2}} \tag{1}$$

for $i = 1, 2,, m$ and $j = 1, 2,\ldots,n$

2. Taking into account the weights assigned to individual features:

$$v_{ij} = w_j \times n_{ij} \tag{2}$$

3. Determining the vector of values of the ideal a^+ and the anti-ideal solution a^-:

$$a^+ = (a_1^+, a_2^+, \ldots, a_n^+) == \left\{\left(\left(\max_{i=1,\ldots,m} v_{ij} \,\middle|\, j \in J_Q\right)\right), \left(\left(\min_{i=1,\ldots,m} v_{ij} \,\middle|\, j \in J_C\right)\right)\right\}$$
$$a^- = (a_1^-, a_2^-, \ldots, a_n^-) == \left\{\left(\left(\min_{i=1,\ldots,m} v_{ij} \,\middle|\, j \in J_Q\right)\right), \left(\left(\max_{i=1,\ldots,m} v_{ij} \,\middle|\, j \in J_C\right)\right)\right\} \tag{3}$$

where: J_Q is the set of stimulants, J_C is the set of destimulants.

4. Calculation of the Euclidean distances of the studied objects from the ideal and anti-ideal solution:

$$d_i^+ = \sqrt{\sum_{j=1}^{n} \left(v_{ij} - a_j^+\right)^2}$$

for $i = 1, 2,\ldots, m$ and $j = 1, 2,\ldots,n$ (4)

$$d_i^- = \sqrt{\sum_{j=1}^{n} \left(v_{ij} - a_j^-\right)^2}$$

for $i = 1, 2,\ldots,m$ and $j = 1, 2,\ldots,n$

5. Determination of the ranking coefficient (closeness coefficient) defining the similarity of objects to the ideal solution:

$$R_i = \frac{d_i^-}{d_i^+ + d_i^-} \tag{5}$$

for $i = 1, 2,\ldots,m$ but $0 \le R_i \le 1$

The highest value of the R_i coefficient indicates the best solution to the considered task [24].

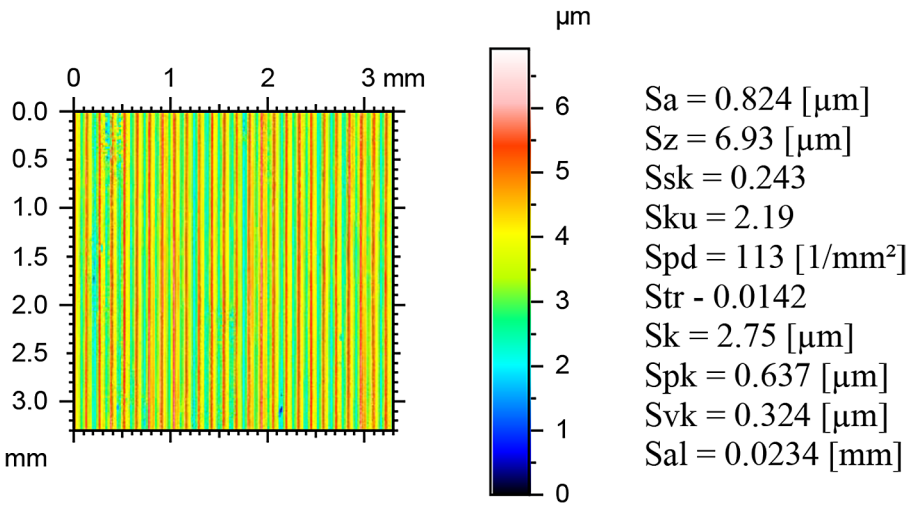

Figure 1. Sample map of turned surface and selected surface topography parameters

RESULTS AND DISCUSSION

The surface after the turning process was an anisotropic surface with a texture aspect ratio (Str) of 0.014. The arithmetic mean surface height (Sa) was 0.769 µm and the maximum surface height (Sz) was 6.84 µm. Following the slide burnishing process, a significant reduction in amplitude parameters was observed. Depending on the burnishing input parameters, the Sa value ranged from 0.068 to 0.294 µm, and the Sz value ranged from 1.64 to 5.14 µm. Kovács et al. [2] noted that this phenomenon results from an increased degree of plastic deformation on the sample surface, which redistributes material from surface peaks to valleys. While the post-burnishing surface remained anisotropic, it showed a slight tendency toward becoming a mixed surface, retaining dominant anisotropic features. The texture aspect ratio Str ranged from 0.096 to 0.365. Parameter values close to 0 but lower than 0.2 indicate an anisotropic nature of the geometric structure, while values close to 1 indicate the opposite trend. The effect of surface smoothing due to slide burnishing is also evident in the surface profile analysis. Figure 2 a, b shows isometric views of turned and burnished (no. 10) surfaces whereas Figure 2 c, d presents example profiles at the same height scale. After burnishing, the surface shape transitioned from one with pointed peaks (Ssk = 0.284 after turning) to a plateau-like structure (Ssk ranging from –0.193 to –1.913). The kurtosis (Sku) increased from 2.19 to values between 3.78 and 6.93, indicating the presence of more pronounced peaks or valleys. For comparison, a perfectly random surface has an Sku of 3. The analysis of the material ratio curve (Figure 2 e, f) also confirms the topographical changes due to burnishing. The core roughness (Sk) of the turned surface decreased from 2.78 µm to 0.227–0.354 µm after the burnishing process, reflecting a smoother, more load-bearing surface.

The reduced peak height (Spk) of the turned surface is relatively high, which indicates the presence of distinct, protruding features. Barmouz and Azarhoushang [25] suggest that higher Spk values indicate an undesirable number of sharp peaks on the surface, which can intensify frictional contact and thus wear.

The reduced valley depth (Svk) also suggests fewer deep depressions after burnishing. Both Spk and Svk values decreased significantly due to the process. Sedlacek et al. [26] emphasized the importance of the Spk/Svk ratio as an indicator of surface quality, which also decreased significantly as a result of burnishing.

The influence of input parameters on surface quality after slide burnishing is illustrated in Figure 3. The data analysis shows that the burnishing force (P) significantly affects all three output parameters. Surface roughness (Sa) decreases as the force increases from 15 N to 120 N, reaching a minimum Sa of 0.068 µm at 120 N. However, further increasing the force to 190 N causes surface quality to deteriorate (Sa increases to 0.294 µm), likely due to local material strain or overload. The residual stresses (σ_{max}) become increasingly compressive with higher burnishing force, reaching a minimum value of –887 MPa at 190 N. This indicates the development of beneficial residual compressive stresses that improve fatigue resistance.

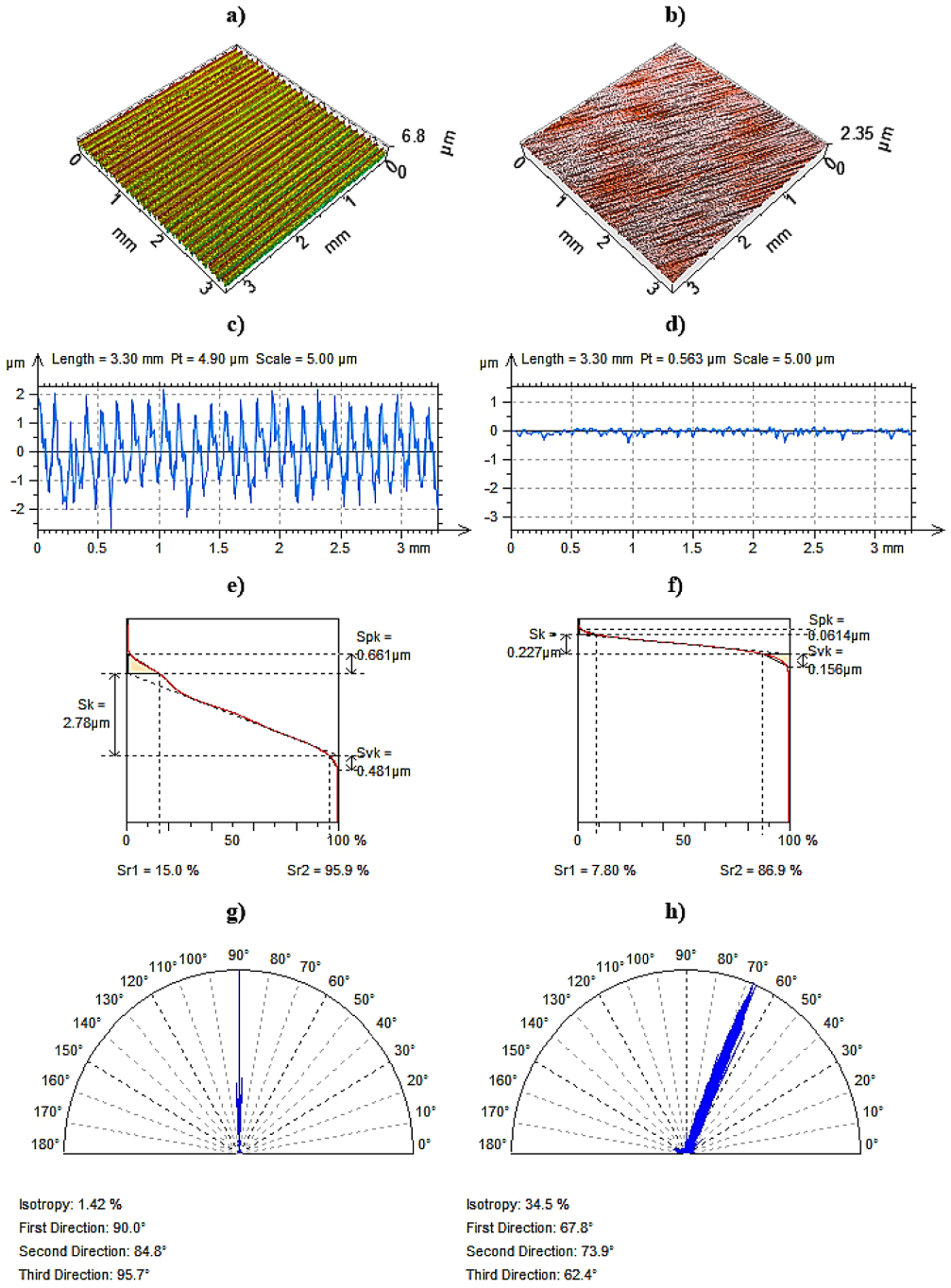

Figure 2. Isometric view (a, b), profile (c, d), Abbott–Firestone curve (e, f) and isotropy rose (g, h) of turned (a, c, e, g) and burnished SB_10 (b, d, f, h) samples

Microhardness (Hm) also increases with burnishing force, reaching the value of 636 HV at 190 N and suggesting significant surface hardening through plastic deformation.

Increasing the feed rate from 0.04 mm/rev to 0.12 mm/rev – while keeping P and n constant – leads to increased surface roughness, which can be explained by the limited number of tool passes per unit length of the material and a lower intensity of the smoothing process. It also leads to a decrease in the value of residual compressive stresses, which are particularly visible at low burnishing force values. Higher feed rates also slightly decrease microhardness. This may be due to reduced material densification in the affected surface layer.

The results indicate that the influence of the rotational speed on the analyzed parameters is less clear compared to the effects of burnishing force or feed rate. Although local variations in the values of surface roughness (Sa), residual stress (σ_{max}),

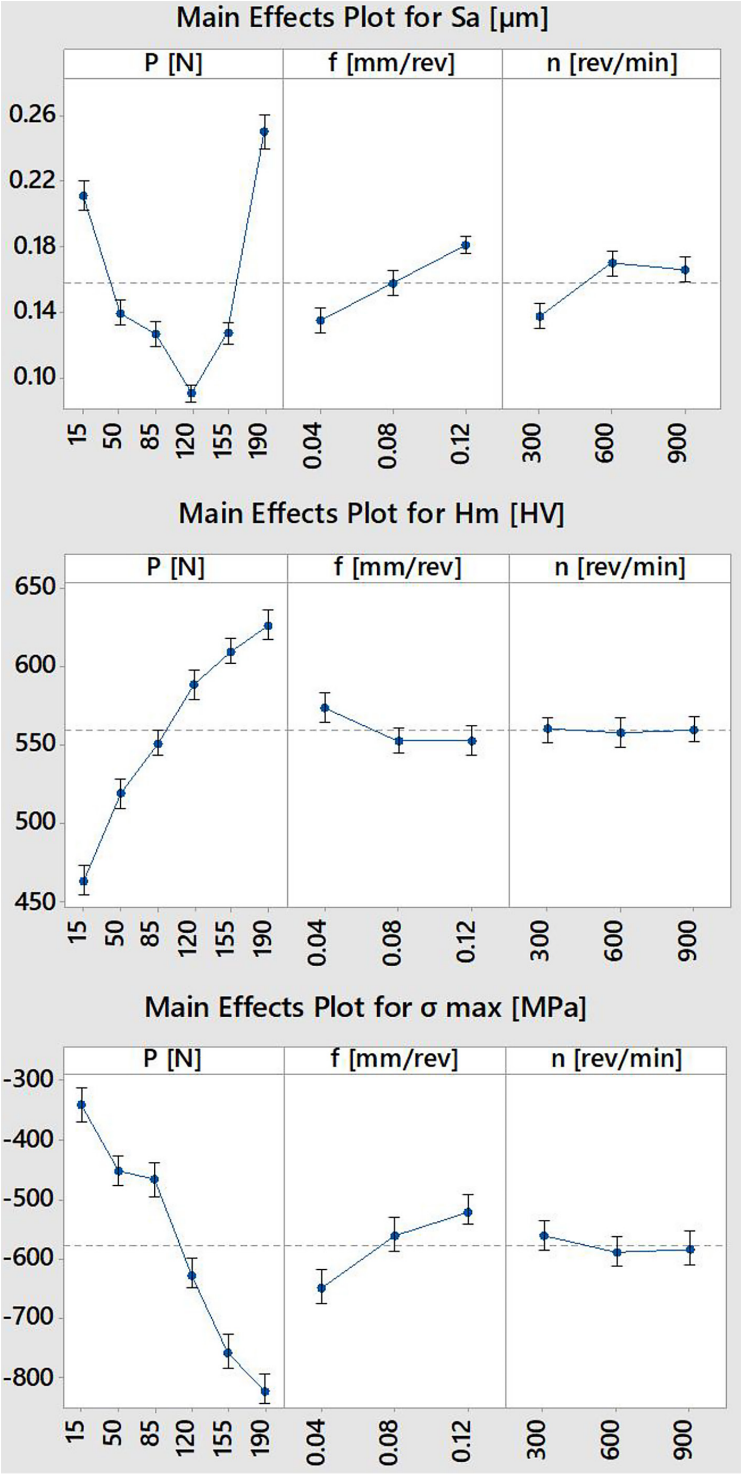

Figure 3. Main effects plots for process input parameters

and microhardness (Hm) are observable, no consistent trend is evident. At higher rotational speeds during the burnishing process, the temperature in the tool – material contact zone increases. Elevated temperatures can lead to localized reductions in hardness and increased material plasticity, which on the one hand facilitates deformation, and on the other hand can weaken the effect of mechanical strengthening. Under certain conditions, this thermal effect may counteract the benefits associated with increased kinetic energy in the process.

To comprehensively evaluate the effectiveness of the slide burnishing process, the TOPSIS method was used. In the evaluation process, surface roughness (Sa) was considered the most critical quality criterion, assigned a weight of 0.4,

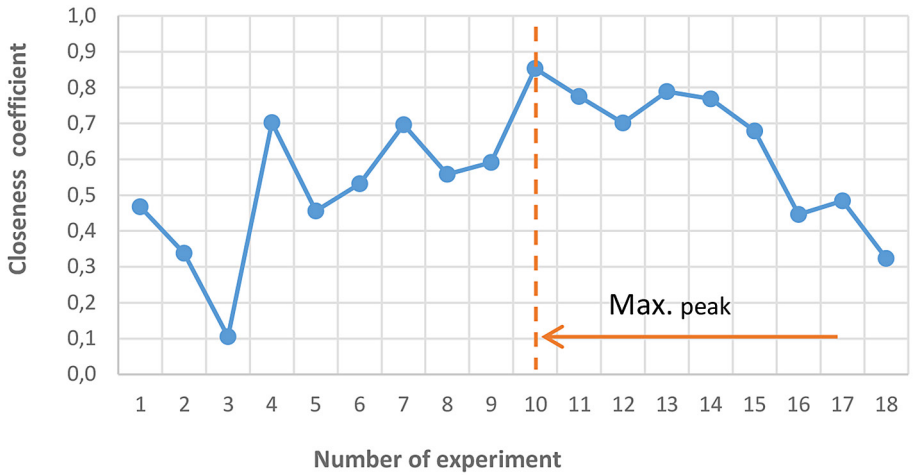

Figure 4. Effect of process parameters in each experiment

Table 2. Values of separation of a positive optimum solution d_i^+, separation of a negative optimum solution d_i^-, closeness coefficient R_i and rank

No.				Rank
SB_01	0.0819	0.0718	0.4672	13
SB_02	0.1009	0.0515	0.3378	16
SB_03	0.1325	0.0156	0.1052	18
SB_04	0.0484	0.1141	0.7023	5
SB_05	0.0822	0.0687	0.4555	14
SB_06	0.0722	0.0821	0.5322	11
SB_07	0.0465	0.1069	0.6966	7
SB_08	0.0673	0.0850	0.5584	10
SB_09	0.0673	0.0974	0.5916	9
SB_10	0.0233	0.1354	0.8530	1
SB_11	0.0355	0.1220	0.7747	3
SB_12	0.0450	0.1056	0.7011	6
SB_13	0.0314	0.1172	0.7885	2
SB_14	0.0337	0.1120	0.7688	4
SB_15	0.0469	0.0991	0.6789	8
SB_16	0.0979	0.0787	0.4457	15
SB_17	0.0824	0.0773	0.4839	12
SB_18	0.1264	0.0605	0.3236	17

due to its direct influence on the tribological and aesthetic properties of the component.

Residual stresses and microhardness were deemed equally important and assigned weights of 0.3 each, given their relevance to fatigue strength and wear resistance. Such a weight distribution reflects a balanced assessment of surface quality from both geometric and mechanical perspectives. Table 2 presents the separation values from the positive optimum solution d_i^+, from the negative optimum solution d_i^-, closeness coefficient R_i and the corresponding ranks, while Figure 4 illustrates the graphical distribution of ranks for various input parameter combinations. The best alternative is chosen based on closeness coefficient.

The best-performing combination, with an R_i = 0.8530, corresponded to the parameters: P = 120 N, f = 0.04 mm/rev, n = 900 rev/min. This variant ranked first due to its low surface roughness (Sa = 0.087 µm) and simultaneously favorable residual stress (–602 MPa) and high microhardness (588 HV) values.

The second-best result was obtained for P = 155 N, f = 0.04 mm/rev, n = 600 rev/min with R_i = 0.7885, followed by P = 120 N, f = 0.08 mm/rev, n = 300 rev/min, which achieved R_i = 0.7747. These variants were characterized by relatively low roughness values, along with high compressive stresses and microhardness. The lowest rated variants included: P = 15 N, f = 0.12 mm/rev, n = 900 rev/min, which achieved the lowest closeness coefficient of R_i = 0.1052 (18th place), and P = 190 N, f = 0.12 mm/rev, n = 600 rev/min, with the value R_i = 0.3236 (17th place). The poor performance of these variants is primarily due to high surface roughness and less favorable values for the other technological parameters.

CONCLUSIONS

Burnishing force proved to be a key parameter determining the surface quality, the state of residual stresses, the microhardness of the surface layer. However, excessive force or feed rate can deteriorate these parameters.

The TOPSIS analysis demonstrated that the optimal slide burnishing results were obtained with moderate burnishing forces (120–155 N) and moderate feed rates (0.08–0.12 mm/rev). Variants with very low force (e.g., 15 N) or high surface roughness were scored poorly, underscoring the importance of selecting appropriate process parameters.

The order determined by the TOPSIS multicriteria decision-making method showed the maximum closeness coefficient value of 0.8530 for experiment no. 10. The corresponding process parameters were: P = 120 N, f = 0.04 mm/rev, n = 900 rev/min.

The ranking based on R_i values clearly indicates the most effective combinations of burnishing parameters with respect to all evaluated criteria. For this reason, the processing parameters corresponding to the highest R_i values are recommended as optimal technological configurations for slide burnishing applications.

The results of this study have practical significance for manufacturing industries and can be directly applied in industrial practice. The optimised parameters of slide burnishing (P = 120–155 N, f = 0.08–0.12 mm/rev, n = 900 rev/min) can be implemented in finishing operations on parts made of 36CrNiMo4 low-alloy steel, such as drive shafts, gear elements, or other highly loaded components. Applying these parameters enables improvement in surface integrity, reduction of friction and wear, and an increase in fatigue strength. The findings provide a practical guideline for selecting effective burnishing conditions in production environments where both surface quality and mechanical durability are required.

Acknowledgments

The study presented in this manuscript was co-financed by the governments of Czechia, Hungary, Poland and Slovakia through Visegrad Fellowship Program of the International Visegrad Fund. The mission of the fund is to promote sustainable regional cooperation in Central Europe. Project No. 62420057.

REFERENCES

1. Zaborski A. Constituting of top layers of enhanced service properties by burnishing working. Tribologia. 2010; 234(6): 271–282.
2. Kovács Z. F., Viharos Z. J., Kodácsy J. Determination of the working gap and optimal machining parameters for magnetic assisted ball burnishing. Measurement. 2018; 118: 172–180. https://doi.org/10.1016/j.measurement.2018.01.033
3. Zaborski A. Analysis of the wear process of surface layers after burnishing. Tribologia. 2022; 299(1): 97-109. https://doi.org/10.5604/01.3001.0015.8988
4. Grabon W., Pawlus P., Galda L., Dzierwa A., Podulka P. Problems of surface topography with oil pockets analysis. J. Phys. Conf. Ser. 2011; 311: 012023. https://doi.org/10.1088/1742-6596/311/1/012023
5. Dzierwa A., Stelmakh N., Tikanashvili N. Application of Taguchi technique to study tribological properties of roller-burnished 36CrNiMo4 steel. Lubricants. 2023; 11: 227. https://doi.org/10.3390/lubricants11050227
6. Zaleski K.. The effect of vibratory and rotational shot peening and wear on fatigue life of steel. Eksploatacja i Niezawodnosc – Maintenance and Reliability. 2017; 19(1): 102–107. https://doi.org/10.17531/ein.2017.1.14
7. Jiménez-García J. I., Capilla-González G., Balvantín-García A. J., Travieso-Rodriguez J. A., Ruíz-López I., Saldaña-Robles A. A numerical investigation into the influence of the slide burnishing process on the real surface roughness and residual stress profiles of AHSS. J. Mater. Res. Technol. 2024; 33: 1406-1419. https://doi.org/10.1016/j.jmrt.2024.09.151 2024
8. Dyl T., Rydz D., Szarek A., Stradomski G., Fik J., Opydo, M. The Influence of slide burnishing on the technological quality of X2CrNiMo17-12-2 steel. Materials. 2024; 17(14): 3403. https://doi.org/10.3390/ma17143403 2024
9. Márquez-Herrera A., Saldaña-Robles A., Reveles-Arredondo J. F., Dorantes-Flores J., Gallardo-Hernandez E. A., Capilla-Gonzalez G. Effect of slide burnishing on the corrosion resistance and surface roughness on high strength steels. Adv. Mech. Eng. 2023; 15(10): 1–10. https://doi.org/10.1177/16878132231201794
10. Tesfom F., Felhő C. Examining the impact of slide burnishing parameters on the 3D surface features of medium carbon steel. J. Prod. Eng.2024; 27(1): 30–35. https://doi.org/10.24867/jpe-2024-01-030
11. Felhő C., Tesfom F., Varga G. ANOVA analysis and L9 Taguchi design for examination of flat slide burnishing of unalloyed structural carbon steel. J. Manuf. Mater. Process. 2023; 7(4): 136. https://doi.org/10.3390/jmmp7040136
12. Zaghal J., Molnár V., Benke M. Improving surface integrity by optimizing slide diamond burnishing parameters after hard turning of 42CrMo4 steel. Int. J. Adv. Manuf. Technol. 2023; 128(5–6): 2087–2103. https://doi.org/10.1007/s00170-023-12008-6

13. Kuznetsov V., Makarov A. I., Skorobogatov A. N., Skorynina P. A., Luchko S. N., Sirosh V. O., Chekan N. S.. Normal force influence on smoothing and hardening of steel 03Cr16Ni15Mo3Ti1 surface layer during dry diamond burnishing with spherical indenter. Obrabotka Metallov. 2022; 24(1): 6–22. https://doi.org/10.17212/1994-6309-2022-24.1-6-22
14. Korzynski M., Dudek K., Korzynska K. Effect of slide diamond burnishing on the surface layer of valve stems and the durability of the stem-graphite seal friction pair. Appl. Sci. 2023; 13(11): 6392. https://doi.org/10.3390/app13116392
15. Maximov J. T., Duncheva G. V., Anchev A. P., Ganev N., Amudjev I. M., Dunchev V. P. Effect of slide burnishing method on the surface integrity of AISI 316Ti chromium–nickel steel. J. Braz. Soc. Mech. Sci. Eng. 2018; 40(4): 1–14. https://doi.org/10.1007/S40430-018-1135-3
16. Çalışkan H. Selection of boron based tribological hard coatings using multi-criteria decision making methods. Mater. Des. 2013; 50: 742–749. https://doi.org/10.1016/j.matdes.2013.03.059
17. Khan M. M., Nisar M., Hajam M. I. High-stress abrasive wear analysis of in situ tic-reinforced zinc–aluminum composites using integrated Taguchi–TOPSIS method. Adv. Eng. Mater. 2023; 25(11): 2201862. https://doi.org/10.1002/adem.202201862
18. Thirumalvalavan S., Perumal G., Senthilkumar N., Selvarasu S. Enhancing tribological characteristics of titanium Grade-5 alloy through HVOF thermal-sprayed WC-Co nano coatings by TOPSIS and golden jack optimization algorithm. Recent Pat Nanotechnol. 2025; 19(4): 544–567. https://doi.org/10.2174/0118722105306841240808092616
19. PN-EN ISO 25178-2:2012; Geometrical Product Specifications (GPS) – Surface Texture: Areal – Part 2: Terms, Definitions and Surface Texture Parameters. International Organization for Standardization: Geneva, Switzerland, 2012.
20. Dzierwa A., Reizer R., Pawlus P., Grabon, W. Variability of areal surface topography parameters due to the change in surface orientation to measurement direction. Scanning. 2014; 36: 170-183. https://doi.org/10.1002/sca.21115
21. Fitzpatric M. E., Fry A. T., Holdway P., Kandil F. A., Shackleton J. Suominen L. L. Determination of residual stresses by X-ray diffraction – Issue 2. A National Measurement Good Practice Guide No. 52. National Physical Laboratory, Teddington, UK. 2005.
22. Kabir G., Hasin, M. A. A. Comparative analysis of TOPSIS and fuzzy TOPSIS for the evaluation of travel website service quality. Int. J. Qual. Res. 2012; 6(3): 169–185.
23. Khudhir W. S., Abbood M. Q., Shukur J. J. Multi-Criteria Decision Making of abrasive water jet machining process for 2024-T3 alloy using hybrid approach. Advances in Science and Technology Research Journal. 2022; 16(5): 155–62. https://doi.org/10.12913/22998624/154040
24. Kuo T. A modified TOPSIS with a different ranking index. Eur. J. Oper. Res. 2017; 260(1): 152–160. https://doi.org/10.1016/j.ejor.2016.11.052
25. Barmouz M., Azarhoushang B. Development of a customized novel additively manufactured honing tool: Surface integrity and Abbott-Firestone assessment of the honed part. Precis. Eng. 2025; 93: 253–258. https://doi.org/10.1016/j.precisioneng.2025.01.013
26. Sedlacek M., Podgornik B., Vizintin J. Influence of surface preparation on roughness parameters, friction and wear. Wear. 2009; 266: 482–487. https://doi.org/10.1016/j.wear.2008.04.017